Pergamon

PII: S0020–7683(96)00195–3

THE OVERALL RESPONSE OF COMPOSITE MATERIALS WITH INCLUSIONS

LINZHI WU, SONGHE MENG and SHANYI DU

School of Astronautics, Harbin Institute of Technology, Harbin, 150001, P.R. China

Abstract—The elastic field of composite materials with inclusions is presented in terms of the integrals of Green's functions. After averaging the strain and stress fields and performing some manipulations and approximations, we obtain the corresponding effective elastic moduli which are related to the integrals of the two-point correlation function. From the expressions obtained, it can be found that the effective elastic moduli of composite materials with inclusions depend on the moduli of two components, the volume fraction of inclusions, as well as the shape, size and distribution of inclusions, and interactions between them. In contrast to previous works, e.g., the self-consistent method, the differential scheme, the Mori-Tanaka method and the generalized self-consistent method, the present method can analyze the effect of the distribution of inclusions on the overall elastic moduli of composite materials, providing that composite materials have periodic microstructures. Finally, some analyses for the effect of the shape, size and distribution of inclusions on the effective elastic moduli of composite materials are given and comparisons with existing methods and experimental results are also considered and discussed. © 1997 Elsevier Science Ltd.

1. INTRODUCTION

The determination of effective elastic moduli of composite materials with inclusions has been extensively investigated. In dealing with how the material properties of each component and microgeometry influence the overall response of composite materials, a large number of approximate approaches have been proposed since this is an open problem and its analytical solution is impossible. An extensive review on this subject is given by Christensen (1979, 1990), Hashin (1983) and Nemat-Nasser and Hori (1993).

A well-known approximation for the effective properties of composite materials with inclusions is the so-called Self-Consistent Method (SCM). It was first devised by Bruggeman (1935) and has been applied for spheroidal particles by Budiansky (1965) and Hill (1965). Using this model, Wu (1966) has investigated the effect of inclusion shape on the effective properties of a two-phase material; Laws and McLaughlin (1979) and Chou et al. (1980) have analyzed the effect of fiber length on the overall moduli of unidirectional short-fiber composites. As pointed out by Nemat-Nasser and Hori (1993), the SCM seeks to predict the interaction of an inclusion and its neighbouring microstructure (the combined effect of the matrix and other inclusions), while the Generalized Self-Consistent Method (GSCM) includes (in a certain approximate sense) the interaction between the inclusion and the surrounding matrix, as well as the neighbouring microstructure. Some improved versions for the GSCM have been established by Smith (1974), Christensen and Lo (1979) and Siboni and Benveniste (1991).

Another method that is related to the SCM is the Differential Scheme (DS). It appears that this method also was first conceived by Bruggeman (1935), but it was more effectively developed and used by Roscoe (1952). Later, this scheme was applied for the effective elastic moduli of composite materials with spherical inclusions by Boucher (1975), McLaughlin (1977), Norris (1985) and Zimmerman (1991).

The Mori-Tanaka Method (MTM) is an average field scheme that has been established by Mori and Tanaka (1973) and has been used by a number of researchers to predict the effective properties. Using the "strain or stress concentration factor" concept, Benveniste (1987) has given a much more direct and simplified derivation of this method, which is different from the Equivalent Inclusion Method (EIM) (Eshelby, 1957). Mori and Wakashima (1990) have reformulated the EIM and referred to it as a successive iteration

method. Zhao and Weng (1990) have investigated the effective elastic moduli of ribbon-reinforced composites using the Eshelby-Mori-Tanaka theory. Recently, Christensen *et al.* (1992) have shown the range of validity of the Mori-Tanaka method.

In addition to the approximate methods mentioned above, there are some other techniques for the determination of effective elastic moduli for composite materials with periodic microstructures. The equivalent inclusion method has been used for the estimation of the overall properties of composites with periodic microstructures by Nemat-Nasser *et al.* (1982), Nemat-Nasser and Taya (1985), Rodin and Hwang (1991) and Rodin (1993). Using the asymptotic homogenization technique, Meguid and Kalamkarov (1994) have analyzed the overall response of composite materials with a regular structure. Utilizing the technique of integral equation, Wu (1992) and Du and Wu (1993) have investigated the effective elastic moduli of composite materials in which the distributions of spherical and cylindrical inclusions are periodic.

The second section of this paper gives the strain and stress fields in terms of the integrals of Green's functions. After averaging the strain and stress fields and performing some manipulations and approximations, we obtain the effective elastic moduli of composite materials with inclusions, which depend on the integral of the strain Green's function in an infinite elastic space and the corresponding integrals of the two-point correlation function. In the expressions related to the two-point correlation function, the microstructural characteristics of composite materials e.g., the shape, size and distribution of inclusions and interactions between them, are considered. The third section presents the corresponding results for the integrals of the two-point correlation function for ellipsoidal and cylindrical inclusions, respectively. In Section 4, the effective elastic moduli of composite materials with spheroidal, ellipsoidal and cylindrical inclusions are numerically calculated. The effects of microstructural parameters, including the shape, size and distribution of inclusions, on the effective elastic module are discussed and analyzed. Comparisons with existing theories and experimental results are also taken into account. Finally, some conclusions from the present study are summarized in Section 5.

2. THE EFFECTIVE ELASTIC MODULI

Consider an elastic medium of total volume V, containing n inclusions. Following Kunin (1983), the strain and stress fields of inhomogeneous medium with inclusions can be expressed in the following form

$$\varepsilon(\mathbf{x}) = \varepsilon_0(\mathbf{x}) - \sum_{\alpha=1}^{n} \int_V \mathbf{K}_0(\mathbf{x}-\mathbf{x}')\mathbf{C}_{1\alpha}\varepsilon_\alpha(\mathbf{x}')\bar{V}_\alpha(\mathbf{x}')d\mathbf{x}' \tag{1}$$

$$\sigma(\mathbf{x}) = \sigma_0(\mathbf{x}) - \sum_{\alpha=1}^{n} \int_V \mathbf{S}_0(\mathbf{x}-\mathbf{x}')\mathbf{B}_{1\alpha}\sigma_\alpha(\mathbf{x}')\bar{V}_\alpha(\mathbf{x}')d\mathbf{x}' \tag{2}$$

where $\varepsilon_0(\mathbf{x})$ and $\sigma_0(\mathbf{x})$ are the strain and stress fields of homogeneous medium without inclusions under the action of the external force, respectively; $\varepsilon_\alpha(\mathbf{x})$ and $\sigma_\alpha(\mathbf{x})$ are the strain and stress fields within the αth-inclusion, respectively; $\mathbf{C}_{1\alpha}$ and $\mathbf{B}_{1\alpha}$ denote the differences of the elastic moduli and compliance between the αth-inclusion and matrix, respectively; $\mathbf{K}_0(\mathbf{x}-\mathbf{x}')$ and $\mathbf{S}_0(\mathbf{x}-\mathbf{x}')$ represent Green's operators for strain and stress fields, respectively; $\bar{V}_\alpha(\mathbf{x})$ is the characteristic function of the αth-inclusion. For convenience, let us suppose that there is some external force field under which the stress and strain fields in the homogeneous medium $\mathbf{C}_0$ are constants. Thus, both $\varepsilon_0(\mathbf{x})$ and $\sigma_0(\mathbf{x})$ in (1) and (2) are constants and $\varepsilon(\mathbf{x})$ and $\sigma(\mathbf{x})$ are the strain and stress fields of the inhomogeneous elastic medium under the action of the external force assumed above.

For a statistically homogeneous material (Hashin, 1983), the effective elastic moduli are established in terms of the macroscopic stress $\langle\sigma(\mathbf{x})\rangle$ and strain $\langle\varepsilon(\mathbf{x})\rangle$. These quantities

are defined as the volume averages over the total volume V

$$\langle\sigma(\mathbf{x})\rangle = \frac{1}{V}\int_V \sigma(\mathbf{x})d\mathbf{x} \tag{3}$$

$$\langle\varepsilon(\mathbf{x})\rangle = \frac{1}{V}\int_V \varepsilon(\mathbf{x})d\mathbf{x}. \tag{4}$$

The effective elastic moduli of $\mathbf{C}^*$ of composite materials are defined by the relation

$$\langle\sigma(\mathbf{x})\rangle = \mathbf{C}^*\langle\varepsilon(\mathbf{x})\rangle. \tag{5}$$

To solve the overall response of composite materials with inclusions, we assume that the strain field inside each inclusion is uniform, but these fields are different for different inclusions. Averaging eqn (1) and (2) yields

$$\langle\varepsilon(\mathbf{x})\rangle = \varepsilon_0 - \frac{1}{V}\sum_{\alpha=1}^{n}\left[\int_V d\mathbf{x}\int_V \mathbf{K}_0(\mathbf{x}-\mathbf{x}')\bar{V}_\alpha(\mathbf{x}')d\mathbf{x}'\right]\mathbf{C}_{1\alpha}\varepsilon_\alpha \tag{6}$$

$$\langle\sigma(\mathbf{x})\rangle = \sigma_0 - \frac{1}{V}\sum_{\alpha=1}^{n}\left[\int_V d\mathbf{x}\int_V \mathbf{S}_0(\mathbf{x}-\mathbf{x}')\bar{V}_\alpha(\mathbf{x}')d\mathbf{x}'\right]\mathbf{B}_{1\alpha}\mathbf{C}_\alpha\varepsilon_\alpha \tag{7}$$

where $\mathbf{C}_\alpha$ and ε_α are the elastic moduli and strain field of the αth-inclusion, respectively.
Let

$$\mathbf{A}_0 = \int_V \mathbf{K}_0(\mathbf{x}-\mathbf{x}')d\mathbf{x}. \tag{8}$$

As pointed out by Mura (1987), when the solution is applied to inclusion problems, it can be assumed with sufficient accuracy that the materials are infinitely extended since the size of inclusions is relatively small compared to the size of the macroscopic material samples. Since the volume V can be approximated by an infinite body, the integral in eqn (8) depends on the shape of V (see Willis, 1976; Mura, 1987). For the volumes of spherical (or cubical) and cylindrical shapes, Appendices A and B present the corresponding expressions of $\mathbf{A}_0$, respectively. Substitution of (8) into (6) yields

$$\langle\varepsilon(\mathbf{x})\rangle = \varepsilon_0 - \sum_{\alpha=1}^{n} V_\alpha\mathbf{A}_0\mathbf{C}_{1\alpha}\varepsilon_\alpha = \varepsilon_0 - \sum_{\alpha=1}^{n}\mathbf{A}_0\mathbf{C}_{1\alpha}\langle\bar{V}_\alpha(\mathbf{x})\varepsilon_\alpha(\mathbf{x})\rangle \tag{9}$$

where V_α is the volume fraction of the αth-inclusion. According to the definition of $\mathbf{S}_0(\mathbf{x}-\mathbf{x}')$, eqn (7) can similarly be written as

$$\langle\sigma(\mathbf{x})\rangle = \sigma_0 - \sum_{\alpha=1}^{n}\mathbf{D}_0\mathbf{B}_{1\alpha}\mathbf{C}_\alpha\langle\bar{V}_\alpha(\mathbf{x})\varepsilon_\alpha(\mathbf{x})\rangle \tag{10}$$

where $\mathbf{D}_0 = \mathbf{C}_0 - \mathbf{C}_0\mathbf{A}_0\mathbf{C}_0$.

Evidently, when the relation between ε_0 and $\langle\bar{V}_\alpha(\mathbf{x})\varepsilon_\alpha(\mathbf{x})\rangle$ is established, the effective elastic moduli can be determined in terms of eqns (5), (9) and (10). For this purpose,

multiplying both sides of (1) by $\bar{V}_\alpha(\mathbf{x})$ and taking the spatial average, we obtain

$$\langle \bar{V}_\alpha(\mathbf{x})\varepsilon_\alpha(\mathbf{x})\rangle = V_\alpha\varepsilon_0 - \frac{1}{V}\sum_{\beta=1}^{n}\left[\int_V \bar{V}_\alpha(\mathbf{x})d\mathbf{x}\int_V \mathbf{K}_0(\mathbf{x}-\mathbf{x}')\bar{V}_\beta(\mathbf{x}')d\mathbf{x}'\right]\mathbf{C}_{1\beta}\varepsilon_\beta. \tag{11}$$

Since $\mathbf{K}_0(\mathbf{x})$ is an even function (see Mura, 1987) and V can be considered as an infinite body, eqn (11) can be rewritten as

$$\langle \bar{V}_\alpha(\mathbf{x})\varepsilon_\alpha(\mathbf{x})\rangle = V_\alpha\varepsilon_0 - \frac{1}{V}\sum_{\beta=1}^{n}\left[\int_V \bar{V}_\alpha(\mathbf{x}+\mathbf{x}')\,d\mathbf{x}\int_V \mathbf{K}_0(\mathbf{x})\bar{V}_\beta(\mathbf{x}')\,d\mathbf{x}'\right]\mathbf{C}_{1\beta}\varepsilon_\beta$$

$$= V_\alpha\varepsilon_0 - \sum_{\beta=1}^{n}\left[\int_V \mathbf{K}_0(\mathbf{x})\langle \bar{V}_\alpha(\mathbf{x})+(\mathbf{x}')\bar{V}_\beta(\mathbf{x}')\rangle_{\mathbf{x}'}\,d\mathbf{x}\right]\mathbf{C}_{1\beta}\varepsilon_\beta \tag{12}$$

where $\langle \bar{V}_\alpha(\mathbf{x}+\mathbf{x}')\bar{V}_\beta(\mathbf{x}')\rangle_{\mathbf{x}'}$ denotes the volume average of $\bar{V}_\alpha(\mathbf{x}+\mathbf{x}')\bar{V}_\beta(\mathbf{x}')$ with respect to $\mathbf{x}'$ and is called the two-point correlation function. Note that we change the order of integrations in the calculation of (12) and the transformation of variable is used.

For simplicity, set

$$\mathbf{F}_{\alpha\beta} = \frac{1}{V_\beta}\int_V \mathbf{K}_0(\mathbf{x})\langle \bar{V}_\alpha(\mathbf{x}+\mathbf{x}')\bar{V}_\beta(\mathbf{x}')\rangle_{\mathbf{x}'}\,d\mathbf{x} \tag{13}$$

where $\mathbf{F}_{\alpha\beta}$ is a fourth-order tensor which characterizes the microstructure of composite materials. It depends on the shape, size and distribution of inclusions. In the next section, we will calculate the integrals $\mathbf{F}_{\alpha\beta}$ of the two-point correlation function for the aligned ellipsoidal and cylindrical inclusions, respectively.

Substituting (13) into (12) yields

$$\langle \bar{V}_\alpha(\mathbf{x})\varepsilon_\alpha(\mathbf{x})\rangle = V_\alpha\varepsilon_0 - \sum_{\beta=1}^{n}\mathbf{F}_{\alpha\beta}\mathbf{C}_{1\beta}\langle \bar{V}_\beta(\mathbf{x})\varepsilon_\beta(\mathbf{x})\rangle. \tag{14}$$

Letting $\alpha = 1,2,\ldots,n$, eqn (14) becomes a system of $6n$ algebraic equations for $\langle \bar{V}_\alpha(\mathbf{x})\varepsilon_\alpha(\mathbf{x})\rangle$. Thus, from this closed system, we can obtain a formal relation between $\langle \bar{V}_\alpha(\mathbf{x})\varepsilon_\alpha(\mathbf{x})\rangle$ and ε_0, which takes the following form

$$\langle \bar{V}_\alpha(\mathbf{x})\varepsilon_\alpha(\mathbf{x})\rangle = \mathbf{E}_\alpha(\mathbf{C}_{1\beta}, V_\beta, \mathbf{F}_{\beta\gamma})\varepsilon_0 \quad (\beta,\gamma = 1,2,\ldots,n) \tag{15}$$

where $\mathbf{E}_\alpha(\mathbf{C}_{1\beta}, V_\beta, \mathbf{F}_{\beta\gamma})$ is a fourth-order tensor.

Substituting (15) into (9) and (10), we can obtain the effective elastic moduli of composite materials which inclusions

$$\mathbf{C}^* = \mathbf{C}_0 + \sum_{\alpha=1}^{n}\mathbf{C}_{1\alpha}\mathbf{E}_\alpha(\mathbf{C}_{1\beta}, V_\beta, \mathbf{F}_{\beta\gamma})\left[\mathbf{I} - \mathbf{A}_0\sum_{\alpha=1}^{n}\mathbf{C}_{1\alpha}\mathbf{E}_\alpha(\mathbf{C}_{1\beta}, V_\beta, \mathbf{F}_{\beta\gamma})\right]^{-1} \tag{16}$$

with the fourth-order unit tensor $\mathbf{I}$ defined as

$$I_{ijkl} = \frac{1}{2}(\delta_{ik}\delta_{jl}+\delta_{il}\delta_{jk}) \tag{17}$$

where δ_{ij} is the Kronecker delta.

Equation (16) is the most general expression for the effective elastic moduli of composite materials with inclusions. If the details of the microstructure of composite materials are known, we can determine the corresponding effective elastic moduli. Below, we consider

a specific case. When all the inclusions have the same shape and size and their distribution is periodic, eqn (14) can be simplified by summation for α as

$$\sum_{\alpha=1}^{n} \langle \bar{V}_\alpha(\mathbf{x})\varepsilon_\alpha(\mathbf{x}) \rangle = V_f\varepsilon_0 - \sum_{\beta=1}^{n} \left(\sum_{\alpha=1}^{n} \mathbf{F}_{\alpha\beta} \right) \mathbf{C}_1 \langle \bar{V}_\beta(\mathbf{x})\varepsilon_\beta(\mathbf{x}) \rangle \tag{18}$$

where V_f is the volume fraction of inclusions and $\mathbf{C}_1 = \mathbf{C}_{1\alpha}$ ($\alpha = 1, 2, \ldots, n$). Since the volume V can be considered as the infinite elastic body and the size of inclusions is relatively small compared to the macroscopic size, the number of inclusions in the interior is much more than that in the exterior for the statistically homogeneous composite materials. Thus,

$$\sum_{\alpha=1}^{n} \mathbf{F}_{\alpha\beta}$$

according to eqn (13) can be regarded as a constant with the sufficient accuracy so long as the coordinate $\mathbf{x}_\beta$ is situated in the interior of composite materials. In the present paper, the coordinate $\mathbf{x}_\beta$ is chosen as the origin of the coordinate system, which virtually is also the geometric center. Substitution of (18) into (9) and (10) yields

$$\mathbf{C}^* = \mathbf{C}_0 + V_f\mathbf{C}_1 \left[\mathbf{I} + \sum_{\alpha=1}^{n} \mathbf{F}_{\alpha\beta}\mathbf{C}_1 - V_f\mathbf{A}_0\mathbf{C}_1 \right]^{-1}. \tag{19}$$

In the fourth section, we will calculate the effective elastic moduli of composite materials with ellipsoidal and cylindrical inclusions according to this expression, respectively. Some detailed "import" and "export" information will be shown and discussed there.

3. THE DETERMINATION OF $\mathbf{F}_{\alpha\beta}$

In this section, we confine our attention to aligned ellipsoidal and cylindrical inclusions, respectively, and assume that all the inclusions have the same shape and size. To determine the integrals $\mathbf{F}_{\alpha\beta}$ of the two-point correlation function, we first give the concrete expression of Green's function $\mathbf{K}_0(\mathbf{x})$ for strain. Following Kunin (1983) and Mura (1987), $\mathbf{K}_0(\mathbf{x})$ can be expressed as

$$[\mathbf{K}_0(\mathbf{x})]_{ijkl} = \frac{1}{8\pi\mu_0(\lambda_0+2\mu_0)|\mathbf{x}|^3} \left[(\lambda_0+3\mu_0)\left(\delta_{ik}\delta_{jl} - \frac{3\delta_{ik}x_jx_l}{|\mathbf{x}|^2} \right) \right.$$
$$\left. - (\lambda_0+\mu_0)\left(2\delta_{l(k}\delta_{i)j} - \frac{12\delta_{i(k}x_{l)}x_j}{|\mathbf{x}|^2} - \frac{3\delta_{jl}x_ix_k}{|\mathbf{x}|^2} + \frac{15x_ix_jx_kx_l}{|\mathbf{x}|^4} \right) \right]_{(ij)(kl)} \tag{20}$$

where λ_0 and μ_0 are the Lame constants, $|\mathbf{x}| = (x_1^2 + x_2^2 + x_3^2)^{1/2}$ and

$$\delta_{l(k}\delta_{i)j} = (\delta_{kl}\delta_{ij} + \delta_{il}\delta_{jk})/2 \tag{21}$$

$$\delta_{i(k}x_{l)}x_j = (\delta_{kl}x_ix_j + \delta_{il}x_jx_k + \delta_{jk}x_ix_l + \delta_{ij}x_kx_l)/4. \tag{22}$$

Next, we solve the two-point correlation function $\langle \bar{V}_\alpha(\mathbf{x}+\mathbf{x}')\bar{V}_\beta(\mathbf{x}') \rangle_{\mathbf{x}'}$ and $\mathbf{F}_{\alpha\beta}$ for aligned ellipsoidal and cylindrical inclusions, respectively.
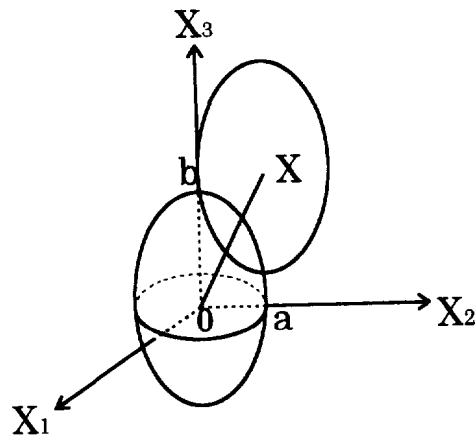
Fig. 1. The relation of $\langle V_\beta(\mathbf{x}+\mathbf{x}')V_\beta(\mathbf{x}')\rangle_{\mathbf{x}'}$ and $\mathbf{x}$ for the ellipsoidal inclusion.

3.1. The ellipsoidal inclusions

As shown in Fig. 1, the ellipsoidal inclusion is described by

$$f(\mathbf{x}) = \frac{x_1^2}{a^2} + \frac{x_2^2}{a^2} + \frac{x_3^2}{b^2} \leqslant 1 \tag{23}$$

where a and b are the principal half axes of the ellipsoid and $t = b/a$ is called the inclusion aspect ratio.

For the case $\alpha = \beta$ as shown in Fig. 1, we have

$$\langle \bar{V}_\beta(\mathbf{x}+\mathbf{x}')\bar{V}_\beta(\mathbf{x}')\rangle_{\mathbf{x}'} = V_\beta J_\beta(\mathbf{x}) \tag{24}$$

where $J_\beta(\mathbf{x})$ is given by

$$J_\beta(\mathbf{x}) = \begin{cases} \left(1 - \dfrac{\sqrt{f(\mathbf{x})}}{2}\right)^2 \left(1 + \dfrac{\sqrt{f(\mathbf{x})}}{4}\right) & f(\mathbf{x}) < 4 \\ 0 & f(\mathbf{x}) \geqslant 4 \end{cases} \tag{25}$$

Since $J_\beta(\mathbf{x})$ possesses the ellipsoidal symmetry, the non-zero components of $\mathbf{F}_{\beta\beta}$ according to Wu and McCullough (1977) and eqn (13) can be written as

$$(F_{\beta\beta})_{1111} = (F_{\beta\beta})_{2222} = \frac{h_1(t)}{2\mu_0} - \frac{3(\lambda_0 + \mu_0)}{8\mu_0(\lambda_0 + 2\mu_0)}h_3(t)$$

$$(F_{\beta\beta})_{3333} = \frac{h_2(t)}{\mu_0} - \frac{\lambda_0 + \mu_0}{\mu_0(\lambda_0 + 2\mu_0)}h_5(t)$$

$$(F_{\beta\beta})_{1122} = (F_{\beta\beta})_{2211} = -\frac{\lambda_0 + \mu_0}{8\mu_0(\lambda_0 + 2\mu_0)}h_3(t)$$

$$(F_{\beta\beta})_{1133} = (F_{\beta\beta})_{3311} = (F_{\beta\beta})_{2233} = (F_{\beta\beta})_{3322} = -\frac{\lambda_0 + \mu_0}{2\mu_0(\lambda_0 + 2\mu_0)}h_4(t)$$

$$(F_{\beta\beta})_{1313} = (F_{\beta\beta})_{2323} = \frac{1}{4\mu_0}\left(\frac{h_1(t)}{2} + h_2(t)\right) - \frac{\lambda_0 + \mu_0}{2\mu_0(\lambda_0 + 2\mu_0)}h_4(t)$$

$$(F_{\beta\beta})_{1212} = [(F_{\beta\beta})_{1111} - (F_{\beta\beta})_{1122}]/2 \tag{26}$$

where $h_i(t)$'s are given by

(1)

$$h_1(t) = \frac{t^2}{1-t^2}\left\{\left[\left(\frac{1-t^2}{t^2}\right)^{1/2} + \left(\frac{t^2}{1-t^2}\right)^{1/2}\right]\tan^{-1}\left(\frac{1-t^2}{t^2}\right)^{1/2} - 1\right\}$$

$$h_2(t) = \frac{1}{1-t^2}\left\{1 - \left(\frac{t^2}{1-t^2}\right)^{1/2}\tan^{-1}\left(\frac{1-t^2}{t^2}\right)^{1/2}\right\}$$

$$h_3(t) = \left(\frac{t^2}{1-t^2}\right)^2\left\{1 + \frac{1}{2t^2} + \left[\frac{1}{2}\left(\frac{1-t^2}{t^2}\right)^{3/2} - \left(\frac{1-t^2}{t^2}\right)^{1/2} - \frac{3}{2}\left(\frac{t^2}{1-t^2}\right)^{1/2}\right]\tan^{-1}\left(\frac{1-t^2}{t^2}\right)^{1/2}\right\}$$

$$h_4(t) = \frac{t^2}{(1-t^2)^2}\left\{-\frac{3}{2} + \left[\frac{1}{2}\left(\frac{1-t^2}{t^2}\right)^{1/2} + \frac{3}{2}\left(\frac{t^2}{1-t^2}\right)^{1/2}\right]\tan^{-1}\left(\frac{1-t^2}{t^2}\right)^{1/2}\right\}$$

$$h_5(t) = \frac{1}{(1-t^2)^2}\left\{1 + \frac{t^2}{2} - \frac{3}{2}\left(\frac{t^2}{1-t^2}\right)^{1/2}\tan^{-1}\left(\frac{1-t^2}{t^2}\right)^{1/2}\right\}$$

(27)

for $0 \leqslant t < 1$;

(2)

$$h_1(1) = 2/3, \quad h_2(1) = 1/3, \quad h_3(1) = 8/15, \quad h_4(1) = 2/15, \quad h_5(1) = 1/5 \qquad (28)$$

for $t = 1$;

(3)

$$h_1(t) = \frac{t^2}{t^2-1}\left\{1 - \frac{1}{2}\left[\left(\frac{t^2}{t^2-1}\right)^{1/2} - \left(\frac{t^2-1}{t^2}\right)^{1/2}\right]\ln\frac{t+(t^2-1)^{1/2}}{t-(t^2-1)^{1/2}}\right\}$$

$$h_2(t) = \frac{1}{t^2-1}\left\{-1 + \frac{1}{2}\left(\frac{t^2}{t^2-1}\right)^{1/2}\ln\frac{t+(t^2-1)^{1/2}}{t-(t^2-1)^{1/2}}\right\}$$

$$h_3(t) = \left(\frac{t^2}{t^2-1}\right)^2\left\{1 + \frac{1}{2t^2} + \left[\frac{1}{4}\left(\frac{t^2-1}{t^2}\right)^{3/2} + \frac{1}{2}\left(\frac{t^2-1}{t^2}\right)^{1/2} - \frac{3}{4}\left(\frac{t^2}{t^2-1}\right)^{1/2}\right]\ln\frac{t+(t^2-1)^{1/2}}{t-(t^2-1)^{1/2}}\right\}$$

$$h_4(t) = \frac{t^2}{(t^2-1)^2}\left\{-\frac{3}{2} + \left[\frac{3}{4}\left(\frac{t^2}{t^2-1}\right)^{1/2} - \frac{1}{4}\left(\frac{t^2-1}{t^2}\right)^{1/2}\right]\ln\frac{t+(t^2-1)^{1/2}}{t-(t^2-1)^{1/2}}\right\}$$

$$h_5(t) = \frac{t^2}{(t^2-1)^2}\left\{1 + \frac{t^2}{2} - \frac{3}{4}\left(\frac{t^2}{t^2-1}\right)^{1/2}\ln\frac{t+(t^2-1)^{1/2}}{t-(t^2-1)^{1/2}}\right\}$$

(29)

for $t > 1$.

For $\alpha \neq \beta$, the two-point correlation function $\langle \bar{V}_\alpha(x+x')\bar{V}_\beta(x')\rangle_{x'}$ can similarly be expressed as

$$\langle \bar{V}_\alpha(x+x')\bar{V}_\beta(x')\rangle_{x'} = \begin{cases} V_\beta\left(1 - \frac{\sqrt{f(x-x_\alpha)}}{2}\right)^2\left(1 + \frac{\sqrt{f(x-x_\alpha)}}{4}\right) & f(x-x_\alpha) < 4 \\ 0 & f(x-x_\alpha) \geqslant 4 \end{cases} \qquad (30)$$

where x_α is the vector connecting the origin ($x_\beta = 0$) of the coordinate system and the center of the αth-inclusion. Letting $y = A(x - x_\alpha)$ where A is a second-order tensor and its non-
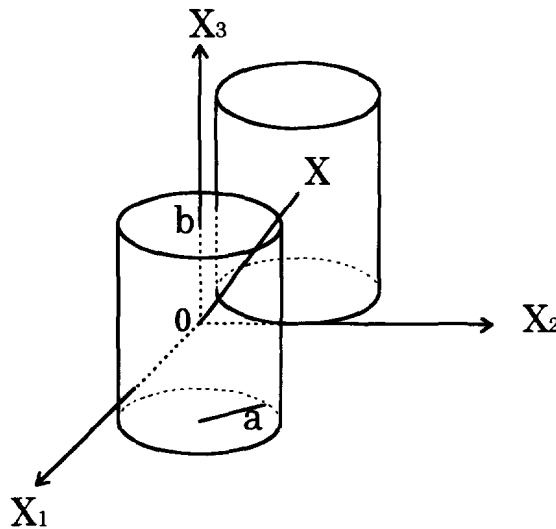
Fig. 2. The relation of $\langle V_\beta(\mathbf{x}+\mathbf{x}')V_\beta(\mathbf{x}')\rangle_{\mathbf{x}'}$ and $\mathbf{x}$ for the cylindrical inclusion.

zero components are as follows

$$A_{11} = A_{22} = 1/a, \quad A_{33} = 1/b \tag{31}$$

and according to (13), we have

$$\mathbf{F}_{\alpha\beta} = \int_{|\mathbf{y}|\leqslant 2} \mathbf{K}_0(\mathbf{x}_\alpha + \mathbf{A}^{-1}\mathbf{y})\left(1 - \frac{|\mathbf{y}|}{2}\right)^2\left(1 + \frac{|\mathbf{y}|}{4}\right)\mathbf{A}^{-1}\mathrm{d}\mathbf{y}. \tag{32}$$

Introducing the polar coordinates

$$y_1 = r\sin\theta\cos\phi, \quad y_2 = r\sin\theta\sin\phi, \quad y_3 = r\cos\theta \tag{33}$$

and substituting (33) into (32) yields

$$\mathbf{F}_{\alpha\beta} = a^2 b\int_0^{2\pi}\mathrm{d}\phi\int_0^\pi \sin\theta\,\mathrm{d}\theta\int_0^2 \mathbf{K}_0(\mathbf{x}_\alpha + \mathbf{A}^{-1}\mathbf{y})\left(1 - \frac{r}{2}\right)^2\left(1 + \frac{r}{4}\right)r^2\,\mathrm{d}r. \tag{34}$$

It should be noted that the vector $\mathbf{x}_\alpha + \mathbf{A}^{-1}\mathbf{y}$ is composed of three components $(x_{\alpha 1} + ar$ $\sin\theta\cos\phi,\ x_{\alpha 2} + ar\sin\theta\sin\phi,\ x_{\alpha 3} + br\cos\theta)$. Integrating with respect to variable r, we can obtain the corresponding analytical expressions but we will not give their concrete expressions due to lengthiness and complexity.

3.2. The cylindrical inclusions

For the case $\alpha = \beta$ as shown in Fig. 2, we have

$$\langle V_\beta(\mathbf{x}+\mathbf{x}')V_\beta(\mathbf{x}')\rangle_{\mathbf{x}'} = V_\beta J_\beta(\mathbf{x}) \tag{35}$$

where $J_\beta(\mathbf{x})$ is given by

$$J_\beta(\mathbf{x}) = \begin{cases} \dfrac{2}{\pi}\left[\cos^{-1}\left(\dfrac{r}{2a}\right) - \dfrac{r}{2a}\sqrt{1 - \left(\dfrac{r}{2a}\right)^2}\right]\left(1 - \dfrac{|z|}{2b}\right) & |z| < 2b \text{ and } r < 2a \\ 0 & |z| \geqslant 2b \text{ and(or) } r \geqslant 2a. \end{cases} \tag{36}$$

Here, (r, θ, z) are the cylindrical coordinates of the vector $\mathbf{x}$, which are relative to the

rectangular Cartesian coordinate system $ox_1x_2x_3$ and a and $2b$ are the radius and height of the cylindrical inclusion, respectively. It should be shown that there are relations between two coordinate systems

$$x_1 = r\cos\theta, \quad x_2 = r\sin\theta, \quad x_3 = z. \tag{37}$$

Substitution of (35) and (36) into (13) and integrations with respect to variables θ and z lead to the following non-zero components

$$(F_{\beta\beta})_{1111} = (F_{\beta\beta})_{2222} = \frac{1}{4\pi\mu_0(\lambda_0+2\mu_0)}\int_0^{2a}\left[2(\mu_0-\lambda_0)H_1 + 6(2\lambda_0+\mu_0)r^2H_2\right.$$

$$\left. -\frac{45}{4}(\lambda_0+\mu_0)r^4H_3\right]\left[\cos^{-1}\left(\frac{r}{2a}\right)-\frac{r}{2a}\sqrt{1-\left(\frac{r}{2a}\right)^2}\right]r\,dr$$

$$(F_{\beta\beta})_{3333} = \frac{1}{2\pi\mu_0(\lambda_0+2\mu_0)}\int_0^{2a}\left[(\mu_0-\lambda_0)H_1 + 6(2\lambda_0+\mu_0)H_4 - 15(\lambda_0+\mu_0)H_5\right]$$

$$\times\left[\cos^{-1}\left(\frac{r}{2a}\right)-\frac{r}{2a}\sqrt{1-\left(\frac{r}{2a}\right)^2}\right]r\,dr$$

$$(F_{\beta\beta})_{1122} = (F_{\beta\beta})_{2211} = \frac{\lambda_0+\mu_0}{4\pi\mu_0(\lambda_0+2\mu_0)}\int_0^{2a}\left[-2H_1 + 6r^2H_2 - \frac{15}{4}r^4H_3\right]$$

$$\times\left[\cos^{-1}\left(\frac{r}{2a}\right)-\frac{r}{2a}\sqrt{1-\left(\frac{r}{2a}\right)^2}\right]r\,dr$$

$$(F_{\beta\beta})_{1133} = (F_{\beta\beta})_{3311} = (F_{\beta\beta})_{2233} = (F_{\beta\beta})_{3322} = \frac{\lambda_0+\mu_0}{4\pi\mu_0(\lambda_0+2\mu_0)}\int_0^{2a}\left[-2H_1 + 3r^2H_2\right.$$

$$\left. +6H_4 - 15r^2H_6\right]\left[\cos^{-1}\left(\frac{r}{2a}\right)-\frac{r}{2a}\sqrt{1-\left(\frac{r}{2a}\right)^2}\right]r\,dr$$

$$(F_{\beta\beta})_{1212} = [(F_{\beta\beta})_{1111} - (F_{\beta\beta})_{1122}]/2$$

$$(F_{\beta\beta})_{1313} = (F_{\beta\beta})_{2323} = \frac{1}{8\pi\mu_0(\lambda_0+2\mu_0)}\int_0^{2a}[4\mu_0H_1 + 3\lambda_0r^2H_2 + 6\lambda_0H_4$$

$$-30(\lambda_0+\mu_0)r^2H_6]\left[\cos^{-1}\left(\frac{r}{2a}\right)-\frac{r}{2a}\sqrt{1-\left(\frac{r}{2a}\right)^2}\right]r\,dr \tag{38}$$

where

$$H_1 = \frac{r^2+4b^2}{br^2(r^2+4b^2)^{1/2}} - \frac{1}{br} \qquad H_2 = \frac{r^2+8b^2}{3br^4(r^2+4b^2)^{1/2}} - \frac{1}{3br^3}$$

$$H_3 = \frac{3r^4+48r^2b^2+128b^4}{15br^6(r^2+4b^2)^{3/2}} - \frac{1}{5br^5} \qquad H_4 = \frac{2r^2+4b^2}{3br^2(r^2+4b^2)^{1/2}} - \frac{2}{3br}$$

$$H_5 = \frac{8r^4+48r^2b^2+48b^4}{15br^2(r^2+4b^2)^{3/2}} - \frac{8}{15br} \qquad H_6 = \frac{2r^2+12r^2b^2+32b^4}{15br^4(r^2+4b^2)^{3/2}} - \frac{2}{15br^3}. \tag{39}$$
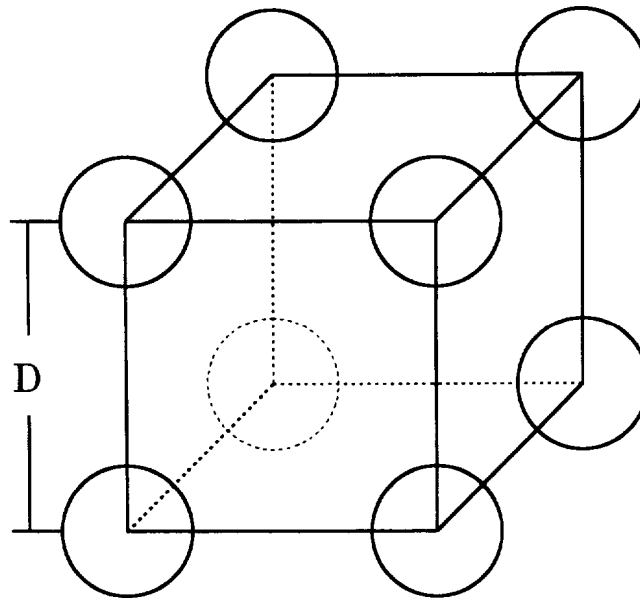
Fig. 3. The simple cubic distribution of spheroidal inclusions.

For $\alpha \neq \beta$, a similar derivation is carried out. From (36), $\langle \bar{V}_\alpha(\mathbf{x}+\mathbf{x}') \bar{V}_\beta(\mathbf{x}') \rangle_{\mathbf{x}'}$ can be written as

$$\langle \bar{V}_\alpha(\mathbf{x}+\mathbf{x}') \bar{V}_\beta(\mathbf{x}') \rangle_{\mathbf{x}'} =$$

$$\begin{cases} \dfrac{2}{\pi}\left[\cos^{-1}\left(\dfrac{r}{2a}\right) - \dfrac{r}{2a}\sqrt{1-\left(\dfrac{r}{2a}\right)^2}\right]\left(1 - \dfrac{|x_3 - x_{\alpha 3}|}{2b}\right) & |x_3 - x_{\alpha 3}| < 2b \text{ and } r < 2a \\ 0 & |x_3 - x_{\alpha 3}| \geqslant 2b \text{ and(or) } r \geqslant 2a \end{cases} \tag{40}$$

where

$$r = [(x_1 - x_{\alpha 1})^2 + (x_2 - x_{\alpha 2})^2]^{1/2} \tag{41}$$

and $(x_{\alpha 1}, x_{\alpha 2}, x_{\alpha 3})$ is the coordinate of the geometrical center of the αth-inclusion. Letting

$$x_1 = x_{\alpha 1} + r\cos\theta, \quad x_2 = x_{\alpha 2} + r\sin\theta, \quad x_3 = x_{\alpha 3} + z, \tag{42}$$

by substituting (40)–(42) into (13) we have

$$\mathbf{F}_{\alpha\beta} = \frac{2}{\pi}\int_0^{2\pi} \mathrm{d}\theta \int_0^{2a} r\,\mathrm{d}r \int_{-2b}^{2b} \mathbf{K}_0(\mathbf{x})\left[\cos^{-1}\left(\frac{r}{2a}\right) - \frac{r}{2a}\sqrt{1-\left(\frac{r}{2a}\right)^2}\right]\left(1 - \frac{|z|}{2b}\right)\mathrm{d}z. \tag{43}$$

Really, integrations with respect to variable z can analytically be solved, but due to the complexity of formulae, we do not give their expressions.

Since $\mathbf{F}_{\alpha\beta}$ can be numerically calculated, the effective elastic moduli of composite materials with aligned ellipsoidal and cylindrical inclusions can be determined in terms of eqn (19) when the distribution of inclusions is known. In Section 4, we will analyze the effect of the shape, size and distribution of inclusions on the overall response of composite materials with periodic microstructures.

4. ANALYSES AND DISCUSSIONS

4.1. *Preliminaries*

In this paper, four different distributions of spheroidal, ellipsoidal and cylindrical inclusions are considered in Figs 3–6. As shown in Fig. 3, the effective elastic properties of
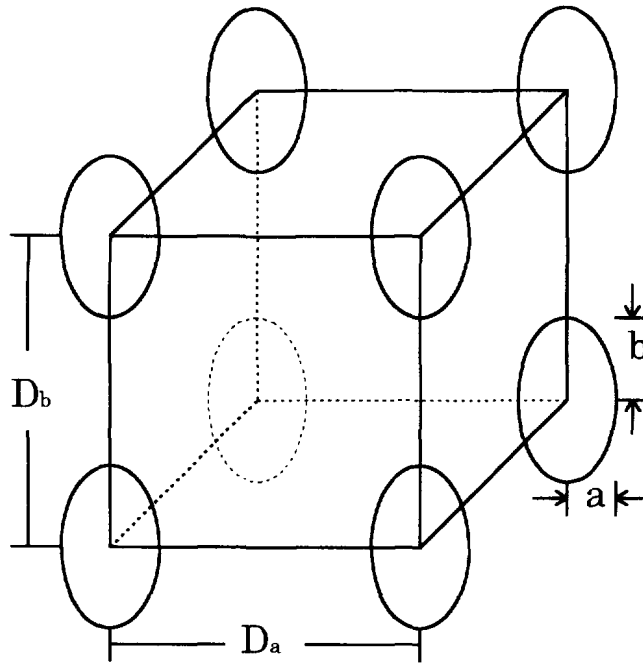
Fig. 4. The periodic microstructure of ellipsoidal inclusions: distribution I.

composite materials can be described by the effective Young's modulus E^* and shear modulus G^*. For ellipsoidal and cylindrical inclusions shown in Figs 4–6, composite materials, as a whole, are transversely isotropic. The five independent effective elastic moduli associated with such a composite are the effective longitudinal Young's modulus E_3^*, longitudinal shear modulus G_{13}^*, G_{23}^*, transverse Young's modulus E_1^*, transverse shear modulus G_{12}^* and transverse bulk modulus κ^*.

From eqn (19), it can be found that the effective elastic moduli of composite materials are related to the tensors $\mathbf{A}_0$ and $\mathbf{F}_{\beta\beta}$ and the summation term

$$\sum_{\alpha=1,\alpha\neq\beta}^{n} F_{\alpha\beta}.$$

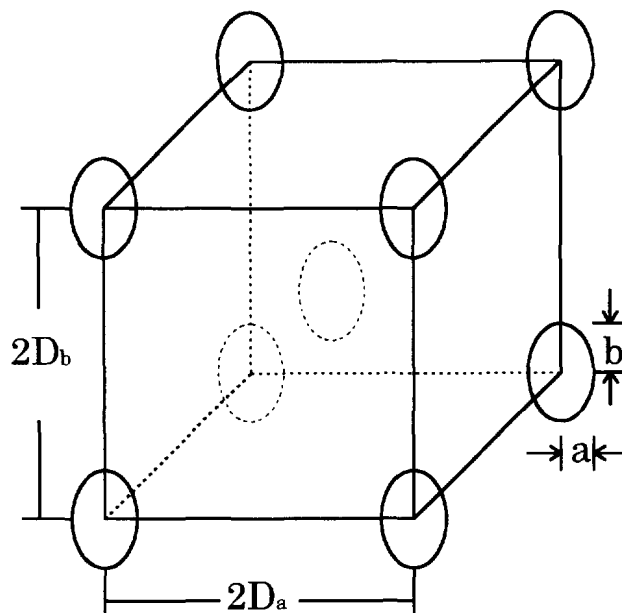For this purpose, we here show the details of solving these tensors indicated above. For the

Fig. 5. The periodic microstructure of ellipsoidal inclusions: distribution II.
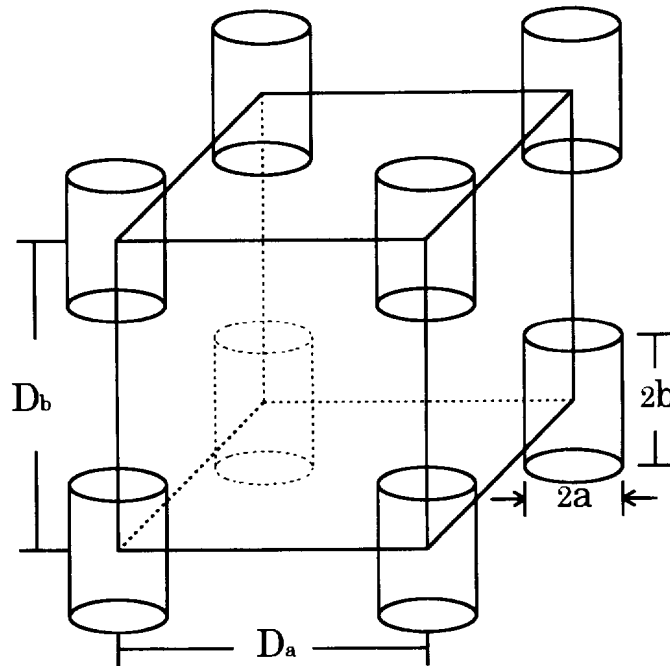
Fig. 6. The periodic distribution of cylindrical inclusions.

simple cubic distribution of spheroidal inclusions as shown in Fig. 3, the tensors A_0 and $F_{\beta\beta}$ are given by Appendix A and eqns (26) and (28), respectively, and $F_{\alpha\beta}(\alpha \neq \beta)$ is determined by (34). In addition, in calculating

$$\sum_{\alpha=1,\alpha\neq\beta}^{n} F_{\alpha\beta},$$

the effect of all the inclusions satisfying $R_{\alpha\beta} \leq 10D$ on the βth-inclusion is taken into account. Here, $R_{\alpha\beta}$ is the distance between the geometrical center of the αth-inclusion and that of the βth-inclusion. (Note that the geometrical center of the βth-inclusion is really the origin of the coordinate system.) For the convergence of numerical results, it can be found from the calculation that when $R_{\alpha\beta} \leq 4D$, numerical results have already converged.

For ellipsoidal and cylindrical inclusions shown in Figs 4–6, A_0 is given by Appendix B. However, the determination of the tensor $F_{\beta\beta}$ and summation term

$$\sum_{\alpha=1,\alpha\neq\beta}^{n} F_{\alpha\beta},$$

is different for the different shape and distribution of inclusions. For the case corresponding to Figs 4 and 5, $F_{\beta\beta}$ is expressed by (26) and (27) for oblate spheroidal inclusions, or (26) and (29) for prolate spheroidal ones. However, for the cylindrical inclusions shown in Fig. 6, $F_{\beta\beta}$ can be obtained in terms of (38) and (39). In Section 3, the calculations of $F_{\alpha\beta}(\alpha \neq \beta)$ for ellipsoidal and cylindrical inclusions have already been given. They correspond to (34) for ellipsoidal inclusions and (43) for cylindrical ones, respectively. It should be shown that in calculating the summation term

$$\sum_{\alpha=1,\alpha\neq\beta}^{n} F_{\alpha\beta},$$

the effect of all the inclusions that satisfy the relations $Z_{\alpha\beta} \leq mD_b$ and $R_{\alpha\beta} \leq mD_s$ on the βth-inclusion is considered. Here, $Z_{\alpha\beta}$ and $R_{\alpha\beta}$ are the longitudinal and radial distances of the geometrical center of the αth-inclusion relative to one of the βth-inclusion, respectively.
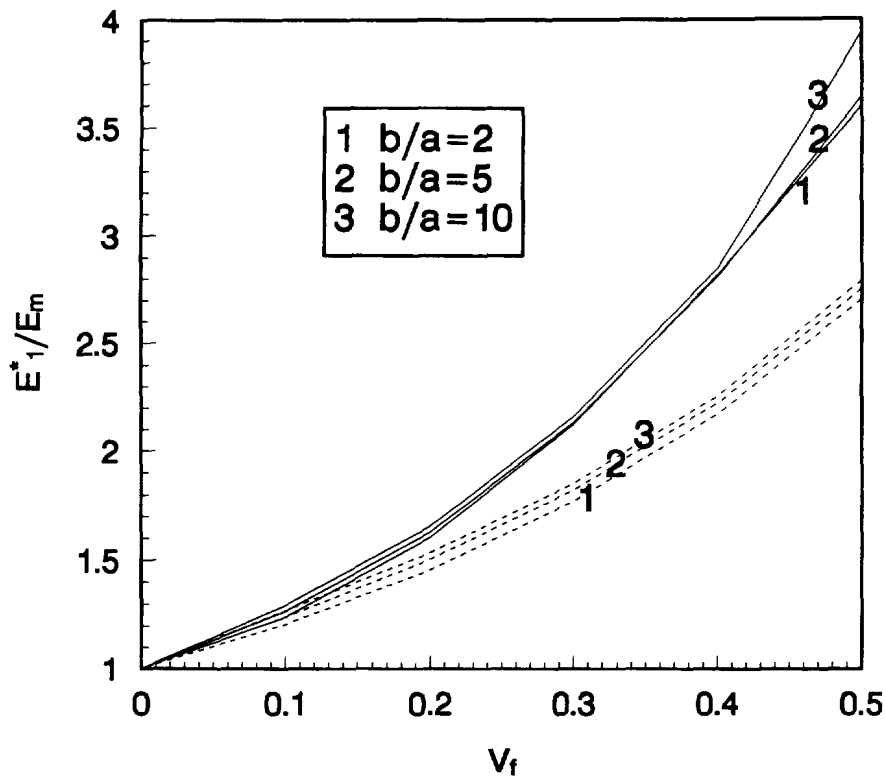
Fig. 7. The variation of E_1^*/E_m with the inclusion volume fraction V_f and aspect ratio b/a for ellipsoidal (solid) and cylindrical (dash) inclusions.

For Figs 4, 5 and 6, m is chosen as 15, 20 and 15 in the present calculation, respectively. Really, when m equals 9 and 12, respectively, the numerical results corresponding to Figs 4 and 5 have already converged. Yet for cylindrical inclusions, the convergence of numerical calculations is relatively poor.

To pave the way in the subsequent analysis, it is necessary to give the elastic constants of each component and the definition of the microstructural parameter e_f. In this paper, the material properties of each component used in the calculation are chosen as $E_f/E_m = 25$, $v_f = 0.23$ and $v_m = 0.39$ for spheroidal inclusions and $E_f/E_m = 20$, $v_f = 0.3$ and $v_m = 0.4$ for ellipsoidal and cylindrical inclusions to compare with some conventional methods and experimental results given by Smith (1975). Here, the subscripts f and m are for the inclusions and matrix, respectively. The microstructural parameter e_f in Fig. 4 is defined as

$$e_f = \frac{D_b - 2b}{D_a - 2a} \tag{44}$$

where a and b are the principal half axes of the ellipsoid and D_a and D_b are the microstructural parameters.

4.2. Numerical results

Below, we will show the effects of the shape, size and distribution of inclusions on the effective elastic moduli of composite materials. Due to the limitation of space, we will only discuss the variations of the effective longitudinal and transverse Young's moduli with the inclusion volume fraction and aspect ratio.

Figure 7 illustrates the variation of the effective transverse Young's modulus E_1^* (normalized by the matrix Young's modulus E_m) with the inclusion volume fraction V_f and the inclusion aspect ratio denoted by b/a. According to this figure, we can find that the shape of inclusions has the significant effect on E_1^*/E_m. However, E_1^*/E_m is not sensitive to the change of the inclusion aspect ratio. This agrees with Halpin and Tsai's report (1967) on the subject.
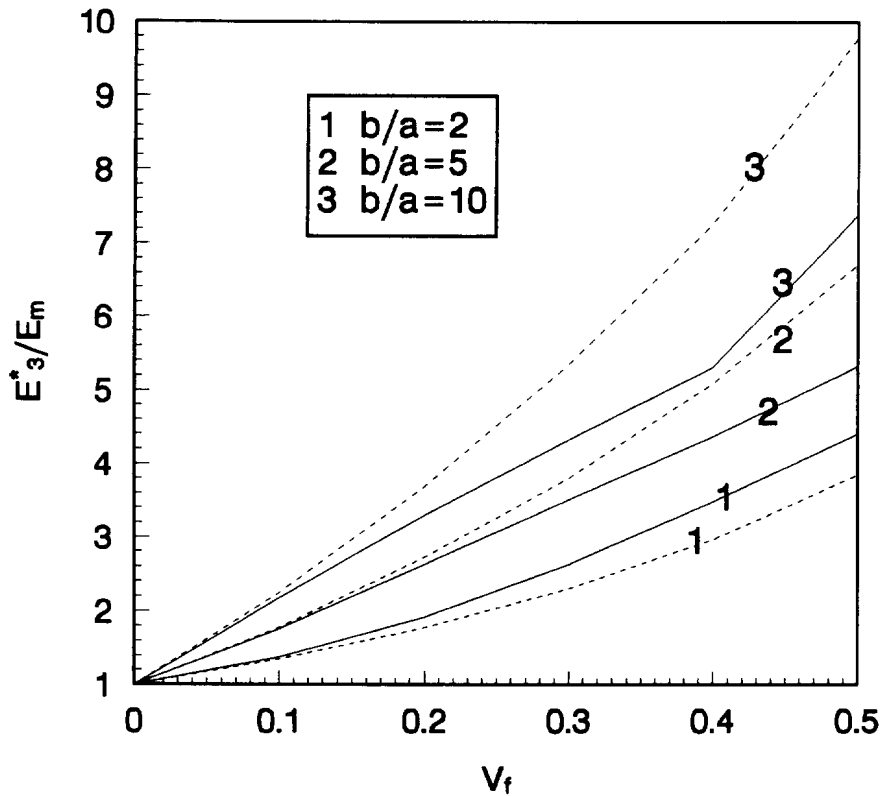
Fig. 8. The variation of E_3^*/E_m with the V_f and b/a for ellipsoidal (solid) and cylindrical (dash) inclusions.

Figure 8 shows the variation of E_3^*/E_m with V_f and b/a. When $b/a = 10$, the effective longitudinal Young's modulus E_3^*/E_m of composite materials with cylindrical inclusions is far larger than the corresponding value of composite materials with ellipsoidal inclusions. However, when $b/a = 5$, the difference between E_3^*/E_m corresponding to cylindrical inclusions and that corresponding to ellipsoidal inclusions becomes small. From the above analysis, we can see that the shape of inclusions has a pronounced effect on the effective modulus E_3^*/E_m when the inclusion aspect ration b/a is larger. It should be shown that the distribution of ellipsoidal inclusions is chosen as the form of Fig. 4 to compare the effect of ellipsoidal and cylindrical inclusions on the effective elastic moduli.

Subsequently, we discuss the effects of the distribution of inclusions and the micro-structural parameter e_f on the effective properties of composite materials. To perform the detailed analyses and comparisons, we confine our attention only to the case of ellipsoidal inclusions. As shown in Fig. 9, the effective transverse Young's modulus E_1^*/E_m is more sensitive to the changes of the inclusion aspect ratio and the distribution of inclusions compared with Fig. 7. This shows that E_1^*/E_m increases when b/a decreases. In addition, it should be noted that the changing curve of E_1^*/E_m for the distribution of Fig. 4 is far higher than that for the distribution of Fig. 5.

Figure 10 gives the results of the present theory and Halpin-Tsai's equation (1967) for $b/a = 0.5$ and 2. Following this figure, we can find that the discrepancy between the present results corresponding to the distribution of Fig. 4 and Halpin-Tsai's equation is very small when $b/a = 2$, but when $b/a = 0.5$ their difference is more pronounced. In addition, it should be noted that the distribution of inclusions has the more pronounced effect on E_3^*/E_m when b/a is smaller.

Except for the different distributions of ellipsoidal inclusions, Figs 11 and 12 illustrate the variations of the effective transverse Young's modulus E_1^*/E_m and longitudinal Young's modulus E_3^*/E_m with V_f for the microstructural parameter $e_f = 0.5, 2, 5$ and 10. It is interesting that the relatively large discrepancy between E_3^*/E_m corresponding to the different micro-structural parameters e_f is at intermediate values of the inclusion volume fraction V_f.
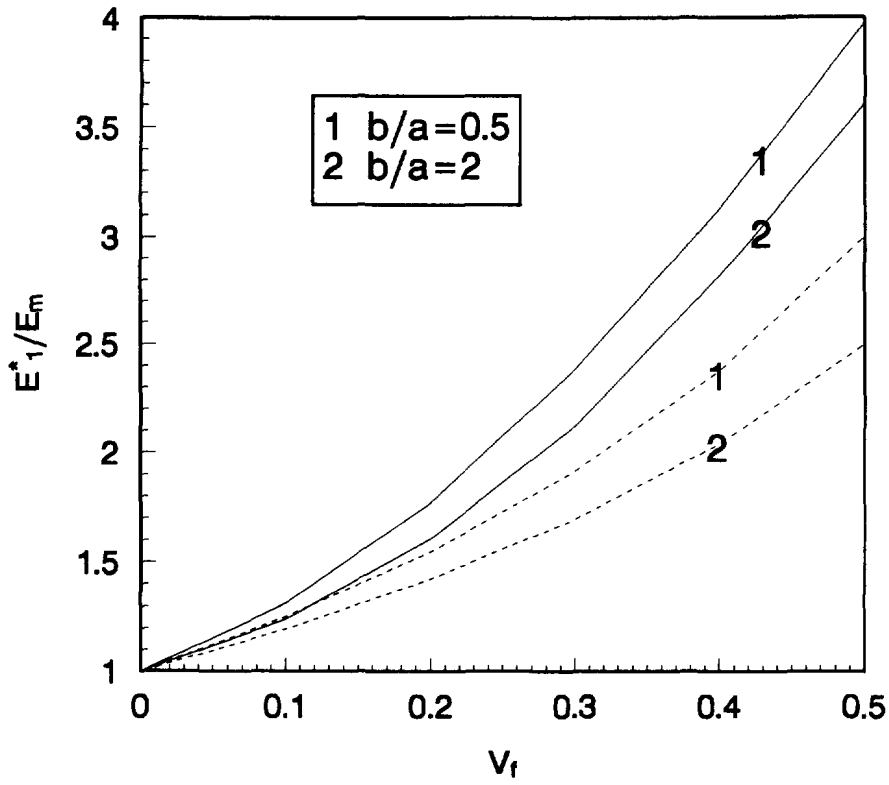
Fig. 9. The variation of E_1^*/E_m with the V_f and b/a for distribution I (solid) and distribution (II) (dash).
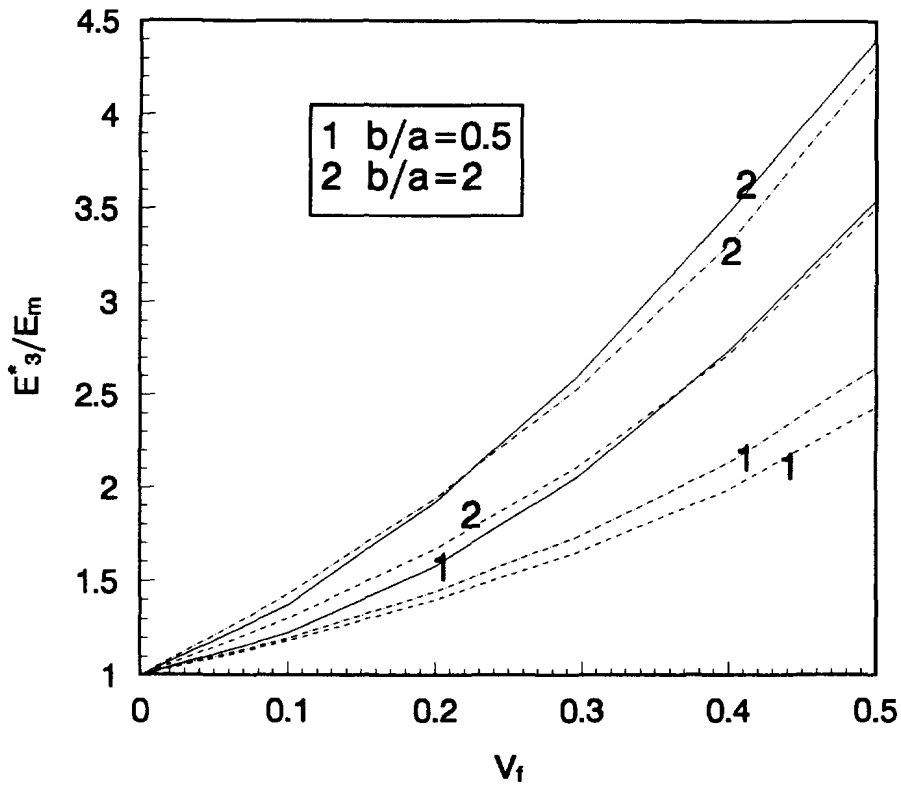

Fig. 10. The variation of E_3^*/E_m with the V_f and b/a for distribution I (solid), distribution (II) (dash) and Halpin-Tsai's equation (dotted-dash).
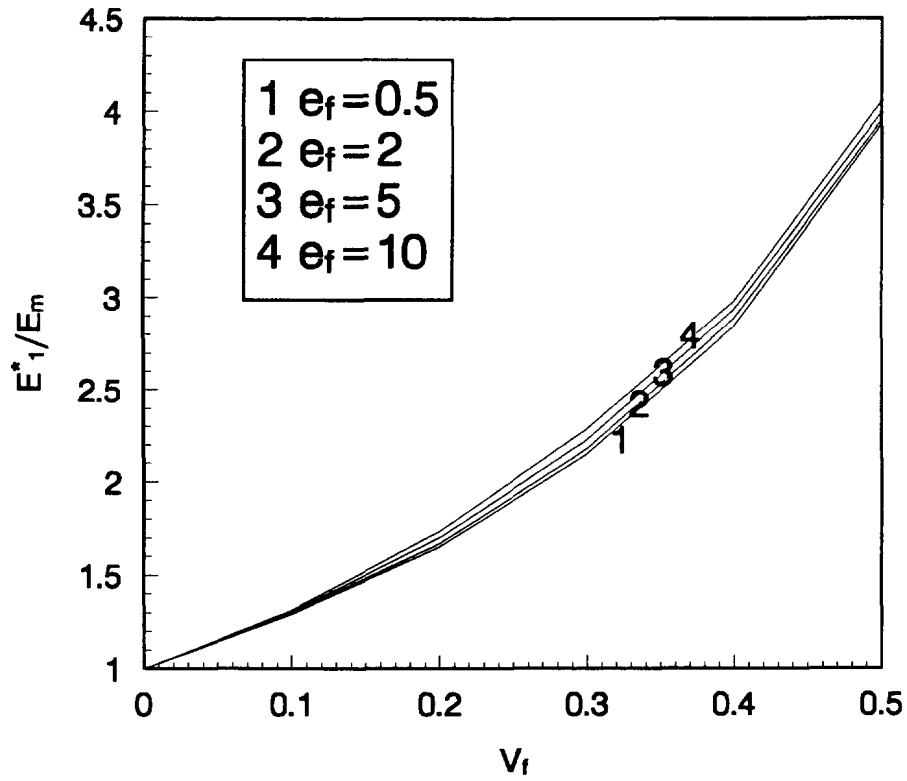
Fig. 11. The variation of E_1^*/E_m with V_f and the microstructural parameter e_f for distribution I.
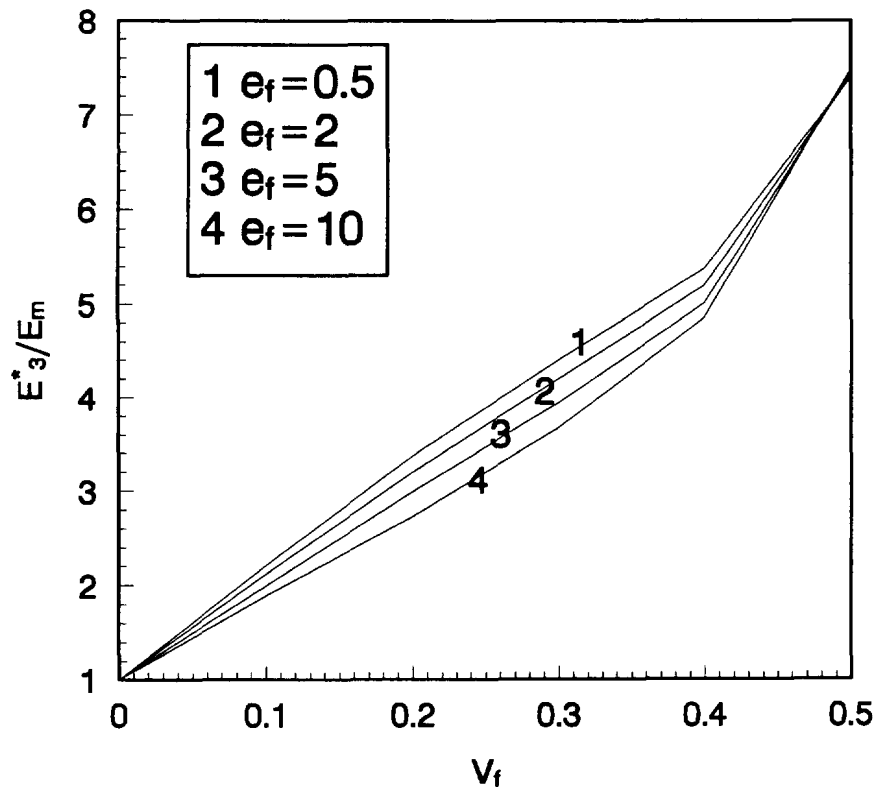

Fig. 12. The variation of E_3^*/E_m with V_f and the microstructural parameter e_f for distribution II.
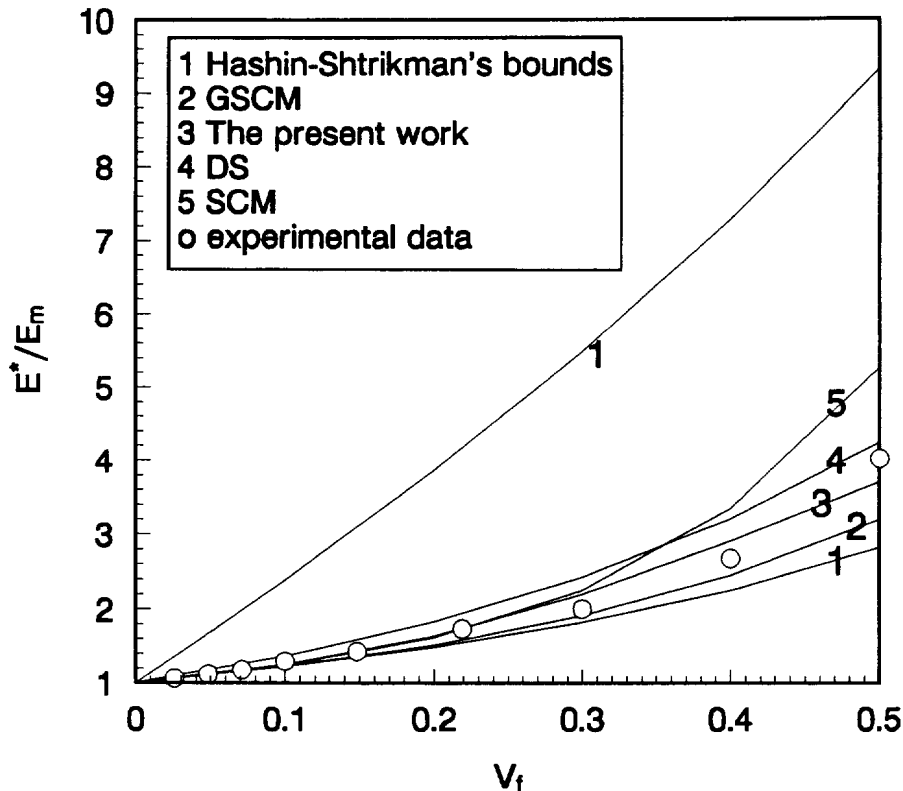
Fig. 13. The variation of E^*/E_m with V_f for spheroidal inclusions.

In order to show the effectiveness of the present theory, Fig. 13 gives the results of the present theory, Hashin and Shtrikman's bounds, the self-consistent method, the differential scheme, the generalized self-consistent method, Mori-Tanaka's method that is the same as Hashin and Shtrikman's lower bound, and the experimental data given by Smith (1975). By comparing with experimental data, we can find that the present theory is effective, particularly when the inclusion volume fraction is larger.

5. CONCLUSIONS

In this paper, the effective elastic moduli of composite materials with aligned ellipsoidal and cylindrical inclusions are derived, respectively. From the expressions obtained, it can be found that the overall properties of composite materials are related to the microgeometry of composite materials, e.g., the shape, size and distribution of inclusions. Particularly, the effect of the distribution of inclusions on the effective properties can effectively be analyzed and investigated by the present method. This case cannot be considered in some conventional theories, e.g., the self-consistent method, the differential scheme, the Mori-Tanaka method and the generalized self-consistent method. In addition, the finite cylindrical inclusion is studied by the present work. According to the authors' knowledge, this problem is not dealt with by the methods mentioned above. However, it should be pointed out that the present work has some limitation because the determination of the effective elastic moduli for composite materials is limited to the case that the distribution of inclusions is periodic.

Following the expressions given in Sections 2 and 3, we calculate the effective elastic moduli of composite materials with spheroidal, ellipsoidal and cylindrical inclusions having periodic distributions, respectively. By comparisons with Halpin-Tsai's equation and analyses, we find that the shape, size and distribution of inclusions have the significant effects on some effective elastic moduli. In comparison with the factors mentioned above, we note that the effect of the change of the microstructural parameter e_f on the effective properties is less. To verify the effectiveness of the present theory, comparisons with some conventional

methods and experimental results are made. From the comparison of results, it can be found that the present theory is more effective since it considers the microgeometry of composite materials with inclusions in detail.

REFERENCES

Benveniste, Y. (1987) A new approach to the application of Mori-Tanaka's theory in composite materials. *Mechanics and Materials*, 6, 147–157.

Boucher, S. (1975) Differential scheme of approximation to compute effective moduli. *Revue M.*, 22, 1.

Bruggeman, D. A. G. (1935) Berechnung verschiedener physikalischer Konstanten von heterogenen Substanzen. I. Dielektrizitaetskonstanten und Leitfaehigkeiten der Mischkoerper aus isotropen Substanzen. *Annalen der Physik*, 24, 636–679 (in German).

Budiansky, B. (1965) On the elastic moduli of some heterogeneous materials. *Journal of Mechanics, Physics and Solids*, 13, 223–227.

Chou, T-W., Nomura, S. and Taya, M. (1980) A self-consistent approach to the elastic stiffness of short-fiber composites. *Journal of Composite Materials*, 14, 178–188.

Christensen, R. M. (1979) *Mechanics of Composite Materials*, Wiley, New York.

Christensen, R. M. (1990) A critical evaluation for a class of micro-mechanics models. *Journal of Mechanics, Physics and Solids*, 38, 379–404.

Christensen, R. M. and Lo, K. H. (1979) Solutions of effective shear properties in three phase sphere and cylinder models. *Journal of Mechanics, Physics and Solids*, 27, 315–330.

Christensen, R. M., Schantz, H. and Shapiro, J. (1992) On the range of validity of the Mori-Tanaka method. *Journal of Mechanics, Physics and Solids*, 40, 69–73.

Du, S. Y. and Wu, L. Z. (1993) Prediction of the overall moduli of a cylindrical short-fiber reinforced composite. *Acta Mechanica Sinica*, 9, 53–60.

Eshelby, J. D. (1957) The determination of the elastic field of an ellipsoidal inclusion, and related problems. *Proceedings of the Royal Society*, A241, 376–396.

Halpin, J. C. and Tsai, S. W. (1967) Environmental factors in composite materials design. *AFML TR67-423*.

Hashin, Z. (1983) Analysis of composite materials—A survey. *Journal of Applied Mechanics*, 50, 481–505.

Hill, R. (1965) A self-consistent mechanics of composite materials. *Journal of Mechanics, Physics and Solids*, 13, 213–222.

Kunin, I. A. (1983) *Elastic Media With Microstructure II*, Springer-Verlag. Berlin.

Laws, N. and McLaughlin, R. (1979) The effect of fiber length on the overall moduli of composite materials. *Journal of Mechanics, Physics and Solids*, 27, 1–13.

McLaughlin, R. (1977) A study of the differential scheme for composite materials. *International Journal of Engineering Science*, 15, 237–244.

Meguid, S. A. and Kalamkarov, A. L. (1994) Asymptotic homogenization of elastic composite materials with a regular structure. *International Journal of Solids and Structures*, 31, 303–316.

Mori, T. and Tanaka, K. (1973) Average stress in matrix and average elastic energy of materials with misfitting inclusions. *Acta Metallurgica*, 21, 571–574.

Mori, T. and Wakashima, K. (1990) Successive iteration method in the evaluation of average fields. In *Micromechanics and Inhomogeneity*, (ed. G. J. Weng, M. Taya and H. Abe), Springer, New York, pp. 269–282.

Mura, T. (1987) *Micromechanics of Defects in Solids*, 2nd ed., Martinus Nijhoff, Dordrecht.

Nemat-Nasser, S. and Hori, M. (1993) *Micromechanics: Overall Properties of Heterogeneous Materials*, North-Holland, Tokyo.

Nemat-Nasser, S., Iwakuma, T. and Hejazi, M. (1982) On composites with periodic structure. *Mechanics and Materials*, 1, 239–267.

Nemat-Nasser, S. and Taya, M. (1985) On effective moduli of an elastic body containing periodically distributed voids: comments and corrections. *Quarterly Applied Mathematics*, 43, 187–188.

Norris, A. N. (1985) A differential scheme for the effective moduli of composites. *Mechanics and Materials*, 4, 1–16.

Rodin, G. J. (1993) The overall elastic response of materials containing spherical inhomogeneities. *International Journal of Solids and Structures*, 30, 1849–1863.

Rodin, G. J. and Hwang, Y.-L. (1991) On the problem of linear elasticity for an infinite region containing a finite number of spherical inhomogeneities. *International Journal of Solids and Structures*, 27, 145–159.

Roscoe, A. N. (1952) The viscosity of suspensions of rigid spheres. *British Journal of Applied Physics*, 3, 267–269.

Siboni, G. and Benveniste, Y. (1991) A micromechanics model for the effective thermomechanical behaviour of multiphase composite media. *Mechanics and Materials*, 11, 107–122.

Smith, J. C. (1974) Correction and extension of van der Poel's method for calculating the shear modulus of a particulate composite. *Journal of the Research National Bureau Standards—A. Physics and Chemistry*, 78A, 355–361.

Willis, J. R. and Acton, J. R. (1976) The overall elastic moduli of a dilute suspension of spheres. *Quarterly Journal of Mechanics and Applied Mathematics*, 29, 163–177.

Wu, C.-T. D. and McCullough, R. L. (1977) Constitutive relationships for heterogeneous materials. In *Developments in Composite Materials*, vol. 1, Applied Science Publishers, 119–187.

Wu, L. Z. (1992) Meso-theory on the elastic media with inclusions and distributed cracks. Ph.D. thesis. Harbin Institute of Technology (in Chinese).

Wu, T. T. (1966) The effect of inclusion shape on the elastic moduli of a two-phase material. *International Journal of Solids and Structures*, 2, 1–8.

Zhao, Y. H. and Weng, G. J. (1990) Effective elastic moduli of ribbon-reinforced composites. *Journal of Applied Mechanics*, **57**, 158–167.
Zimmerman, R. W. (1991) Elastic moduli of a solid containing spherical inclusions. *Mechanics and Materials*, **12**, 17–24.

APPENDIX A

Since the volume V in (8) is regarded as the infinite region, the tensor $\mathbf{A}_0$ according to Wu and McCullough (1977) and Wu (1992) can be expressed in the following form when the shape of V is spheroidal and cuboidal

$$(A_0)_{ijkl} = \frac{3\lambda_0 + 8\mu_0}{15\mu_0(\lambda_0 + 2\mu_0)} I_{ijkl} - \frac{\lambda_0 + \mu_0}{15\mu_0(\lambda_0 + 2\mu_0)} \delta_{ij}\delta_{kl}. \tag{A1}$$

APPENDIX B

As shown in Fig. 2, when V is an infinite cylinder, the integral in (8) can be written as

$$(A_0)_{1111} = (A_0)_{2222} = \frac{1}{8\mu_0(\lambda_0 + 2\mu_0)}\left[(\lambda_0 + 5\mu_0)\frac{t}{(1+t^2)^{1/2}} + \frac{3}{2}(\lambda_0 + \mu_0)\frac{t}{(1+t^2)^{3/2}}\right]$$

$$(A_0)_{3333} = \frac{1}{2\mu_0(\lambda_0 + 2\mu_0)}\left[2\mu_0 + (\lambda_0 - \mu_0)\frac{t}{(1+t^2)^{1/2}} - (\lambda_0 + \mu_0)\frac{t^3}{(1+t^2)^{3/2}}\right]$$

$$(A_0)_{1122} = (A_0)_{2211} = -\frac{\lambda_0 + \mu_0}{8\mu_0(\lambda_0 + 2\mu_0)}\left[\frac{t}{(1+t^2)^{1/2}} - \frac{t}{2(1+t^2)^{3/2}}\right]$$

$$(A_0)_{1133} = (A_0)_{3311} = (A_0)_{2233} = (A_0)_{3322} = -\frac{\lambda_0 + \mu_0}{4\mu_0(\lambda_0 + 2\mu_0)}\frac{t}{(1+t^2)^{3/2}}$$

$$(A_0)_{1212} = [(A_0)_{1111} + (A_0)_{1122}]/2$$

$$(A_0)_{1313} = (A_0)_{2323} = \frac{1}{8\mu_0(\lambda_0 + 2\mu_0)}\left[2(\lambda_0 + 2\mu_0) - (\lambda_0 + 2\mu_0)\frac{t}{(1+t^2)^{1/2}} - 2(\lambda_0 + \mu_0)\frac{t}{(1+t^2)^{3/2}}\right] \tag{B1}$$

where $t = b/a$ is called the inclusion aspect ratio.